ASYMPTOTIC ANALYSIS OF 3D BUOYANT MAGNETOHYDRODYNAMIC FLOWS IN STRONG MAGNETIC FIELDS

L. Bühler, C. Wetzel

Forschungszentrum Karlsruhe, Postfach 3640, 76021 Karlsruhe, Germany
(leo.buehler@iket.fzk.de)

Introduction. In a helium cooled lead lithium blanket for nuclear fusion reactors, the entire fusion power is removed by helium that flows at high pressure and speed inside cooling plates. The liquid metal breeder is confined in cavities formed by the cooling plates and heat conduction dominates the temperature field inside the fluid, subject to a strong, externally applied magnetic field.

For evaluation of three-dimensional buoyant MHD flows, a numerical tool is extended that is based on inertialess asymptotic techniques valid at the high Hartmann numbers occurring in fusion applications. It is assumed in this first step that the temperature equation decouples from the flow problem for the low Péclet numbers that are typical for the considered liquid metal flows. The analysis applies ideas of Kulikovskii [1] to buoyant MHD flows but differs from the formulation by Alboussière [2] who used different coordinates.

1. Formulation. Consider the three-dimensional buoyancy-driven, inertialess, incompressible flow of an electrically conducting viscous fluid subject to an externally applied magnetic field. For strong magnetic fields, i.e. for high Hartmann numbers $\mathrm{Ha} = LB\sqrt{\sigma/(\rho\nu)} \gg 1$, the momentum equation and Ohms law governing the flow outside viscous layers reduce at leading order to

$$\nabla p - \mathbf{f} = \mathbf{j} \times \mathbf{B}, \tag{1}$$

$$\nabla \phi + \mathbf{j} = \mathbf{v} \times \mathbf{B}, \tag{2}$$

with conservation of mass and charge, $\nabla \cdot \mathbf{v} = 0$ and $\nabla \cdot \mathbf{j} = 0$. Here, the variables $\mathbf{B}$, $\mathbf{v}$, $\mathbf{j}$, $\mathbf{f}$, ϕ and p stand for the magnetic field, velocity, current density, buoyancy force, electric potential and pressure, scaled by the reference values B_0, $v_0 = \nu/L\mathrm{Gr}/\mathrm{Ha}^2$, $\sigma v_0 B_0$, $\sigma v_0 B_0^2$, $v_0 L B_0$, and $\sigma v_0 L B_0^2$, respectively. The electric conductivity of the fluid σ and its kinematic viscosity ν are assumed to be constant and the temperature dependent density ρ enters the equations through the Boussinesq approximation in terms of $\mathbf{f} = -T\hat{\mathbf{g}}$. In this formulation T represents the difference between local and reference temperature, scaled by a typical temperature difference ΔT. Inertia remains negligible if $\mathrm{Gr}/\mathrm{Ha}^4 \ll 1$, where the Grashof number $\mathrm{Gr} = g\gamma T L^3/\nu^2$ gives the nondimensional measure for the buoyant forcing in a geometry of typical length L, determined by gravity $g\hat{\mathbf{g}}$ and thermal expansion coe.cient γ.

Viscous effects are confined to thin boundary layers and enter the problem for the flow in the inviscid core exclusively through the electric boundary condition

$$\mathbf{j} \cdot \mathbf{n} = \nabla_t \cdot [(c + \delta)\nabla_t \phi] \tag{3}$$

where the retarded fluid in the boundary layer of thickness $\delta = (\mathrm{Ha}\mathbf{Bn})^{-1}$ contributes to the nondimensional wall conductivity given by the wall conductance ratio $c = \sigma_{\mathrm{w}} d/(\sigma L)$. Here σ_{w} stands for the electric conductivity of the wall with

thickness d, $\mathbf{n}$ is the inward unit normal and ∇_t stands for the gradient opera-
tor in the plane of the wall. Currents which leave the fluid core enter the viscous
boundary layer or the wall, turn in tangential direction and create along the wall a
distribution of potential ϕ that serves as boundary condition for the core equations.
The kinematic condition for core velocity $\mathbf{v} \cdot \mathbf{n} = 0$ is suffcient to determine the
flow in the core. Details of the flow in the viscous layers can be obtained later by a
reconstruction of the well-known viscous Hartmann profile or by a reconstruction
of the flow in parallel layers [3].

2. Analysis. In order to achieve a numerical description that can be ap-
plied to a number of general MHD problems, the governing equations are formu-
lated in curvilinear coordinates, where one coordinate is aligned with the direction
of the magnetic field (along $\hat{z}$). The other two coordinates are boundary fitted to
describe in a special way the surface contour of the duct or cavity. The general
coordinates u^i describe the fluid domain by the mapping

$$x = \bar{\mathbf{x}} \left(u^1, u^2 \right) + h \left(u^1, u^2 \right) u^3 \hat{\mathbf{z}}, \tag{4}$$

in which $\bar{\mathbf{x}}$ represents a *middle* surface in the cavity that divides any magnetic field
line in the duct into two parts of equal length h. The contour of the geometry
is defined by two parts, e.g. the *upper* and the *lower* part for $u^3 = 1$ and $u^3 =
-1$. The equations (1)–(3) are formulated in tensor notation as outlined in [4],
with the additional buoyancy term included. The momentum equation is solved
for two current components while the third one is determined by integrating the
charge conservation equation along magnetic field lines. Now currents have a
representation as a function of pressure gradient $\partial_i p$, buoyancy force f_i, and a yet
unknown integration function α as

$$j^k = j^k \left(\partial_i p - f_i, \alpha \right). \tag{5}$$

Then Ohms law is solved for two velocity components and the third one is ob-
tained by integration of mass conservation along magnetic field lines. The final
representation of velocity reads now

$$v^k = v^k \left(\partial_i \phi + j_i, \beta \right), \tag{6}$$

where the velocity depends on potential gradient $\partial_i \phi$, currents j_i, and a second
integration function β. The two integration functions are expressed in terms of the
wall potentials at the upper and lower wall $\phi \left(u^3 = \pm 1 \right)$. Elimination of current
from (5) and (6) and applying the kinematic boundary condition at the walls yields
a second order partial differential equation for the determination of pressure as a
function of wall-potential gradients. The problem is entirely described by solving
the second order PDE (3) on the walls $u^3 = \pm 1$ for potential, after replacing the
wall normal currents by formulation (5).

The code has been validated at various simple test cases for which solutions
are available. One verification example is the magneto-convection in a long vertical
circular pipe with transverse horizontal magnetic field $\mathbf{B} = \hat{\mathbf{z}}$ and given uniform
horizontal temperature gradient $\nabla T = \hat{\mathbf{y}}$. It is possible to determine by asymptotic
techniques the core velocity along the vertical axis x as

$$\mathbf{v} = y \left(2 + \frac{h\mathrm{Ha}}{\mathrm{chHa} + 1} \right) \hat{\mathbf{x}}, \quad \text{where} h = \sqrt{1 - y^2}. \tag{7}$$

A comparison of the numerically obtained results with this analytical expression
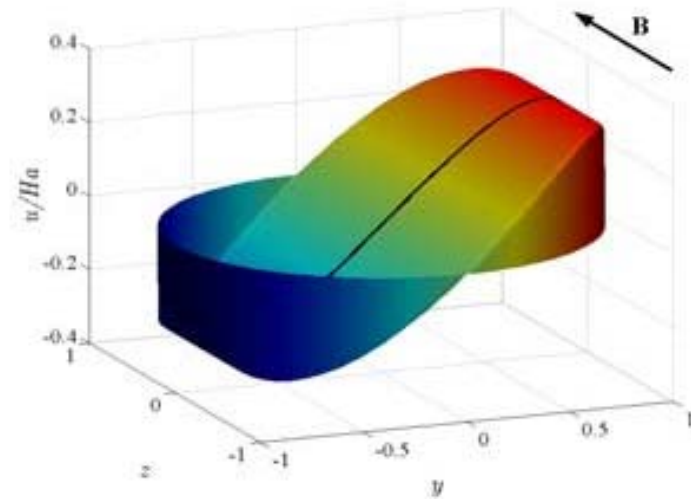gives perfect agreement (see Fig. 1).

Fig. 1. Velocity profile in a long vertical pipe with transverse magnetic field $\mathbf{B} = \hat{\mathbf{z}}$, driven by a non-uniform temperature $T = y$. For comparison with the Eq. (7) see the black line at $z = 0$. Colors indicate temperature.

3. Three-dimensional calculations. As an example for a threedimensional calculation we present the magneto-convective flow in a thermosyphon. We consider a *standing* torus with major radius R and circular cross section of radius $r = 1$. The magnetic field is aligned with the horizontal major axis of the torus, i.e. $\mathbf{B} = \hat{\mathbf{z}}$, and the fluid is subject to a given uniform horizontal temperature gradient $\nabla T = \hat{\mathbf{y}}$ in a vertical gravity field aligned along $-\hat{\mathbf{x}}$. Such temperature profiles lead to a 3D distribution of pressure while the potential exhibits no variation along the toroidal direction as shown in Fig. 2.

Inspection of velocity profiles shows further that the velocity, like the potential, does not change along the toroidal direction. The velocity profile and
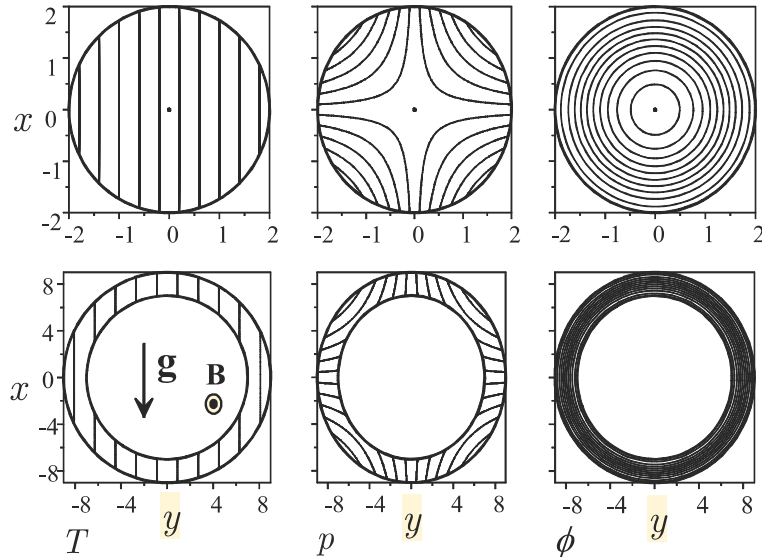

Fig. 2. Magneto-convection in an electrically insulating loop with major radius $R = 1$ (upper) and $R = 8$ (lower row) for Ha = 1000. Surface contours of temperature (first), pressure (second), potential (third column).
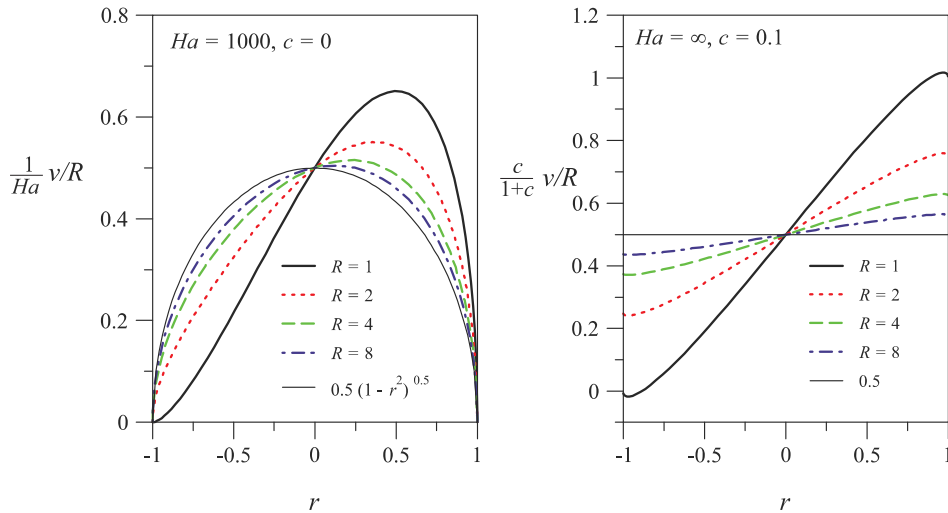
Fig. 3. Azimutal velocity profiles for different major radii R for insulating and conducting walls.

magnitude, however depend essentially on the major radius and on the Hartmann number. This can be seen from Fig. 3. The latter figure shows radial velocity profiles in the equatorial plane of the torus. For Ha $\gg$ 1 this velocity profile is practically constant along magnetic field lines in the whole cross section but decays quickly to zero within the thin Hartmann layers at the wall. For the small major radius $R = 1$ the flow is carried preferentially near the outer region. The reason is obvious since the driving pressure gradient is highest near the outer wall and vanishes at the inner wall that coincides with the major axis of the torus. For larger R the pressure becomes more and more uniform in the cross section and the velocity approaches profiles which are typical for pressure-driven MHD flows in straight insulating pipes, where $v \sim \sqrt{1 - r^2}$ [5]. For conducting walls we find a similar behavior, i.e. higher core velocities in the outer and lower velocities in the inner regions and a tendency that the flow approaches the typical velocity profile as in conducting straight pipe flow as $R \to \infty$, where $v \to$ const.

4. Conclusions. A 3D asymptotic-numeric code has been extended to account for buoyant e.ects in MHD flows at high Hartmann numbers. The code has been tested with several known solutions and applied to the 3D geometry of a toroidal thermosyphon with given temperature profile. For creeping flows at low Peclet numbers, the derived model is flexible enough to be applied for a variety of other geometries and temperature distribution. For flows at higher Peclet numbers one should include in the model additionally the coupling between the flow and the temperature field.

REFERENCES

1. A.G. KULIKOVSKII. Flows of a conducting incompressible liquid in an arbitrary region with a strong magnetic field. *Fluid Dynamics*, vol. 8 (1974), no. 1, pp. 462-467. Russian original (1973).

2. T. ALBOUSSIERE, J.P. GARANDET, R. MOREAU. Asymptotic analysis and symmetry in MHD convection. *Physics of Fluids*, vol. 8 (1996), no. 8, pp. 2215-2226.

3. L. BUHLER. Laminar buoyant magnetohydrodynamic flow in vertical rectangular ducts. *Physics of Fluids*, vol. (1998), no. 1, pp. 223-236.

4. L. BUHLER. Magnetohydrodynamic flows in arbitrary geometries in strong, nonuniform magnetic fields. *Fusion Technology*, vol. 27 (1995), pp. 3-24.

5. J.A. SHERCLIFF. Magnetohydrodynamic pipe flow Part 2. High Hartmann number. *Journal of Fluid Mechanics*, vol. 13 (1962), pp. 513-518.